

Zic2 regulates the expression of Sert to modulate eye-specific refinement at the visual targets

This is an open-access article distributed under the terms of the Creative Commons Attribution Noncommercial Share Alike 3.0 Unported License, which allows readers to alter, transform, or build upon the article and then distribute the resulting work under the same or similar license to this one. The work must be attributed back to the original author and commercial use is not permitted without specific permission.

Cristina García-Frigola and Eloísa Herrera*

Instituto de Neurociencias, Consejo Superior de Investigaciones Científicas & Universidad Miguel Hernandez, Alicante, Spain

The development of the nervous system is a time-ordered and multi-stepped process that requires neural specification, axonal navigation and arbor refinement at the target tissues. Previous studies have demonstrated that the transcription factor Zic2 is necessary and sufficient for the specification of retinal ganglion cells (RGCs) that project ipsilaterally at the optic chiasm midline. Here, we report that, in addition, Zic2 controls the refinement of eye-specific inputs in the visual targets by regulating directly the expression of the serotonin transporter (Sert), which is involved in the modulation of activity-dependent mechanisms during the wiring of sensory circuits. In agreement with these findings, RGCs that express Zic2 ectopically show defects in axonal refinement at the visual targets and respond to pharmacological blockage of Sert, whereas Zic2-negative contralateral RGCs do not. These results link, at the molecular level, early events in neural differentiation with late activity-dependent processes and propose a mechanism for the establishment of eye-specific domains at the visual targets.

The EMBO Journal (2010) 29, 3170–3183. doi:10.1038/emboj.2010.172; Published online 30 July 2010

Subject Categories: development; neuroscience

Keywords: axon refinement; serotonin transporter; visual system; Zic2

Introduction

Sense organs are responsible for the perception of the surrounding environment. During the development of the nervous system, sensory organs have to connect to the appropriate target areas in the brain in order to function normally. The visual system has long been an ideal model system for understanding how development sculpts the organization of sensory circuits. In the visual system of mammals, retinal ganglion cells (RGCs) from each eye diverge at the optic chiasm midline to send axonal projections to the main visual targets—the thalamic lateral geniculate nucleus (LGN)

and the superior colliculus (SC)—at both sides of the brain. In the mouse, most visual fibres cross the midline (contralateral) except for a few axons that arise from the peripheral ventrotemporal (VT) region of the retina that avoid the midline and project instead to the same side of the brain (ipsilateral) (Erskine and Herrera, 2007).

To maintain positional information of the visual fields and allow binocular vision, the final projection pattern of visual fibres at the targets follows two remarkable features: (1) topography along the anteroposterior and the latero-medial axis and (2) eye-specific segregation of ipsilateral and contralateral axons (Godement *et al.*, 1984; Chapman and Stryker, 1993; Chapman *et al.*, 1996; McLaughlin *et al.*, 2003; Huberman *et al.*, 2008). At birth, when RGC axons reach the visual targets, they initially invade the entire SC and LGN (Sretavan *et al.*, 1988; McLaughlin *et al.*, 2003) but after a precise refinement process, the topographic and eye-specific projection pattern are well defined around 2 weeks after birth.

The molecular program that controls early guidance events of retinal axons at the optic chiasm has been described clearly. The transcription factor Zic2 is expressed in uncrossed (iRGCs) but not in crossed (cRGCs) ganglion cells, and is necessary and sufficient to control the expression of the guidance receptor EphB1 (Herrera *et al.*, 2003; García-Frigola *et al.*, 2008). Glial cells at the optic chiasm express EphrinB2, an EphB1 ligand, and the interaction of these two membrane proteins mediates the axonal repulsive response of ipsilateral axons at the midline (Williams *et al.*, 2003).

The molecular mechanisms governing the subsequent steps that visual fibres follow to establish the final projection pattern at their targets are starting to be elucidated. The establishment of topographic maps in both ipsilateral and contralateral fibres is mediated by the tyrosine kinase receptors EphAs and their ligands, the ephrinAs. Mice lacking EphA/ephrinA signalling show defects in axonal mapping at the SC and the thalamus. Mutations in the transmembrane protein, Ten_m3, or in the multi-domain protein Phr1 also lead to defects in the mapping of RGC axons. However, none of these molecules are differentially expressed in iRGC or cRGCs and consequently the segregation of ipsilateral and contralateral fibres in all these mutant mice is not affected (Pfeiffenberger *et al.*, 2005; Leamey *et al.*, 2007; Culican *et al.*, 2009).

In contrast, the refinement of retinal axons is perturbed when neural activity is manipulated. Thus, in mice that lack $\beta 2$ subunits of the neuronal nicotinic acetylcholine receptor, or in ferrets that receive intraocular injections of epibatidine, stage II spontaneous waves are abolished and although axons project to the correct retinotopic location in the targets, they form diffuse axonal arborizations and ipsilateral and contra-

*Corresponding author: Department of Developmental Neurobiology, Instituto de Neurociencias de Alicante (CSIC-UMH), Avd Ramón y Cajal s/n, Alicante 03550, Spain. Tel.: +34 965 919231; Fax: +34 965 919200; E-mail: e.herrera@umh.es

Received: 22 March 2010; accepted: 1 July 2010; published online: 30 July 2010















lateral processes do not segregate properly (Penn *et al*, 1998; Rossi *et al*, 2001). In addition, when serotonin signalling, a well-characterized pathway involved in the modulation of neural activity (Gu and Singer, 1995; Mazer *et al*, 1997; Sarnyai *et al*, 2000; Edagawa *et al*, 2001; Gaspar *et al*, 2003; Sodhi and Sanders-Bush, 2004), is genetically or pharmacologically altered axon refinement and proper axonal arborization are disrupted in the visual and in other sensory systems (Rhoades *et al*, 1993; Arce *et al*, 1995; Bastos *et al*, 1999; Upton *et al*, 1999, 2002; Salichon *et al*, 2001; Butt *et al*, 2002; Xu *et al*, 2004; Gonzalez *et al*, 2008).

Despite the fact that the formation of the visual system in mammals has served as a model for studying axonal navigation at the midline and the coupling of neural sensory inputs in the targets, the molecular connection between both processes has been poorly investigated. Here, we report that the transcription factor Zic2 regulates directly the expression of the serotonin transporter (Sert) in iRGCs to refine eye-specific projections in primary visual targets. These results reveal that the same transcription factor that controls axon guidance in an intermediate target also regulates activity-dependent refinement events at the final targets.

Results

Zic2 and Sert are co-expressed in ipsilateral RGCs

To search for Zic2 target genes, we compared the gene expression profiles of VT retinal segments of embryonic day E16.5. WT and Zic2 mutant embryos (*Zic2^{kd/kd}*) (Nagai *et al*, 2000). Only seven probe sets fulfilled the restrictive criteria applied to identify *bona fide* targets of Zic2 (Figure 1; for further details in microarrays results see Supplementary Figure S1). The only two downregulated genes in the list were the neural precursor cell-expressed, developmentally downregulated gene 9 (*Nedd9/HEF1*) and the serotonin transporter (*Sert*; encoded by *slc6a4*). *Nedd9/HEF1* is a scaffolding protein in the integrin signalling pathway involved in cell adhesion dynamics (O'Neill *et al*, 2000) and may represent an interesting candidate target gene for further study. Here, we focus on Sert, an integral membrane protein responsible for the efficient uptake of serotonin from the extracellular space. This was the most downregulated gene in our analysis (−3.4-fold).

ID probe	WT	Kd	Gene symbol	Average fold	P-values
1417150_at			<i>slc6a4</i>	FC=−3.42;	P=0.001
1422818_at			<i>Nedd9</i>	FC=−2.30;	P=1.9e−4
1437132_x_at			<i>Nedd9</i>	FC=−2.17;	P=0.016
1425286_at			<i>Crygn</i>	FC=4.45;	P=0.04
1434369_a_at			<i>Cryab</i>	FC=4.41;	P=0.0057
1430350_at			2610035F20R	FC=4.24;	P=0.027
1438323_at			<i>Lim2</i>	FC=2.09;	P=0.046

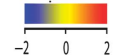


Figure 1 Gene expression analysis comparing VT retinal segments from E16.5 WT and Zic2 mutant retinas. Hit map generated from the DNA microarray data showing the seven probe sets/transcripts (six genes) significantly altered on samples from Zic2 knockdown mice (*Zic2^{kd/kd}*) with fold change larger than 2 ($P < 0.05$, unpaired *t*-test). This graph was generated using the GeneSpring GX software. The probe-set ID (left), gene symbol, average fold change over triplicate microarrays (FC) and *P*-values for each transcript are indicated. The colour scale bar indicates upregulation in red and downregulation in blue.

To evaluate the relationship between Zic2 and Sert, we performed double staining, combining immunohistochemistry against Zic2 and *in situ* hybridization for Sert transcripts, on retinal cryosections from E16.5 mouse embryos. We found that both genes were co-expressed by the same cells in the most peripheral VT segment of the retina (Figure 2A), the location of iRGCs. To investigate whether Sert, like Zic2, is expressed in iRGCs and not in cRGCs, we performed immunostaining for Sert in semi-intact whole-mount preparations of the ventral diencephalon containing the entire optic chiasm region. Sert staining was clearly detectable in retinal axons turning ipsilaterally at the optic chiasm, whereas Sert-positive retinal axons crossing the midline were not observed (Figure 2B). This suggests that Sert is expressed specifically in iRGCs and not in both iRGCs and cRGCs as thought previously (Upton *et al*, 1999).

Next, we compared the temporal expression patterns of Zic2 and Sert at different developmental stages. As described previously, Zic2 expression first appeared in the peripheral VT segment at E14.5 (Herrera *et al*, 2003). Consistent with Zic2 expression, Sert mRNA was detected in the VT retina at this age. At E16.5, when the expression of Zic2 peaked in the VT retina, Sert mRNA also was expressed highly in a domain identical to that of Zic2. At P0, the expression of both genes was found at the very periphery of the VT retina, and by P4 and later stages both molecules were undetectable (Figure 2C). The co-incident spatiotemporal expression of Zic2 and Sert in the mouse retina, together with the expression of Sert in ipsilateral but not in contralateral RGC axons, make this gene an excellent candidate as a Zic2 downstream effector molecule.

Zic2 is necessary and sufficient to induce the expression of Sert

To further test whether Zic2 is required for Sert expression in the VT region of the retina, we examined Sert mRNA levels in Zic2 hypomorphic mutant mice (*Zic2^{kd/kd}*). These mice die around E17.5 and display barely detectable levels of Zic2 (Herrera *et al*, 2003). We therefore examined Sert mRNA expression at E16.5 in *Zic2^{kd/kd}* and wild-type littermates when both Zic2 and Sert expression levels peak in the retina (Figure 2C). Sert mRNA levels were highly reduced in the VT retina of *Zic2^{kd/kd}* embryos compared with WT littermates (Figure 3A). These data indicate that Zic2 expression in the developing neural retina is necessary for the expression of Sert in iRGCs.

Next, we assessed whether Zic2 is sufficient to induce Sert expression *in vivo*. Specific primers were designed to detect Sert mRNA in mouse embryonic retinas by quantitative RT-PCR (qRT-PCR). To validate the primers, dorsonasal (DN) and VT retinal segments were dissected out from E16.5 WT embryos and endogenous levels of Sert mRNA were measured. VT segments showed an increase of around 3.5-fold in Sert mRNA levels compared with segments from the DN region of the retina (Figure 3B). Using the highly efficient *in utero* electroporation protocol developed in our laboratory (García-Frigola *et al*, 2007, 2008), mammalian expression vectors containing EGFP (pCAG-EGFP) or/and Zic2 (pCAG-Zic2)-coding sequences were ectopically introduced into RGCs of the centre of the retina at E13.5 At 1 or 3 days after electroporation, the targeted central portions of the retina were dissected out and Sert mRNA levels measured by

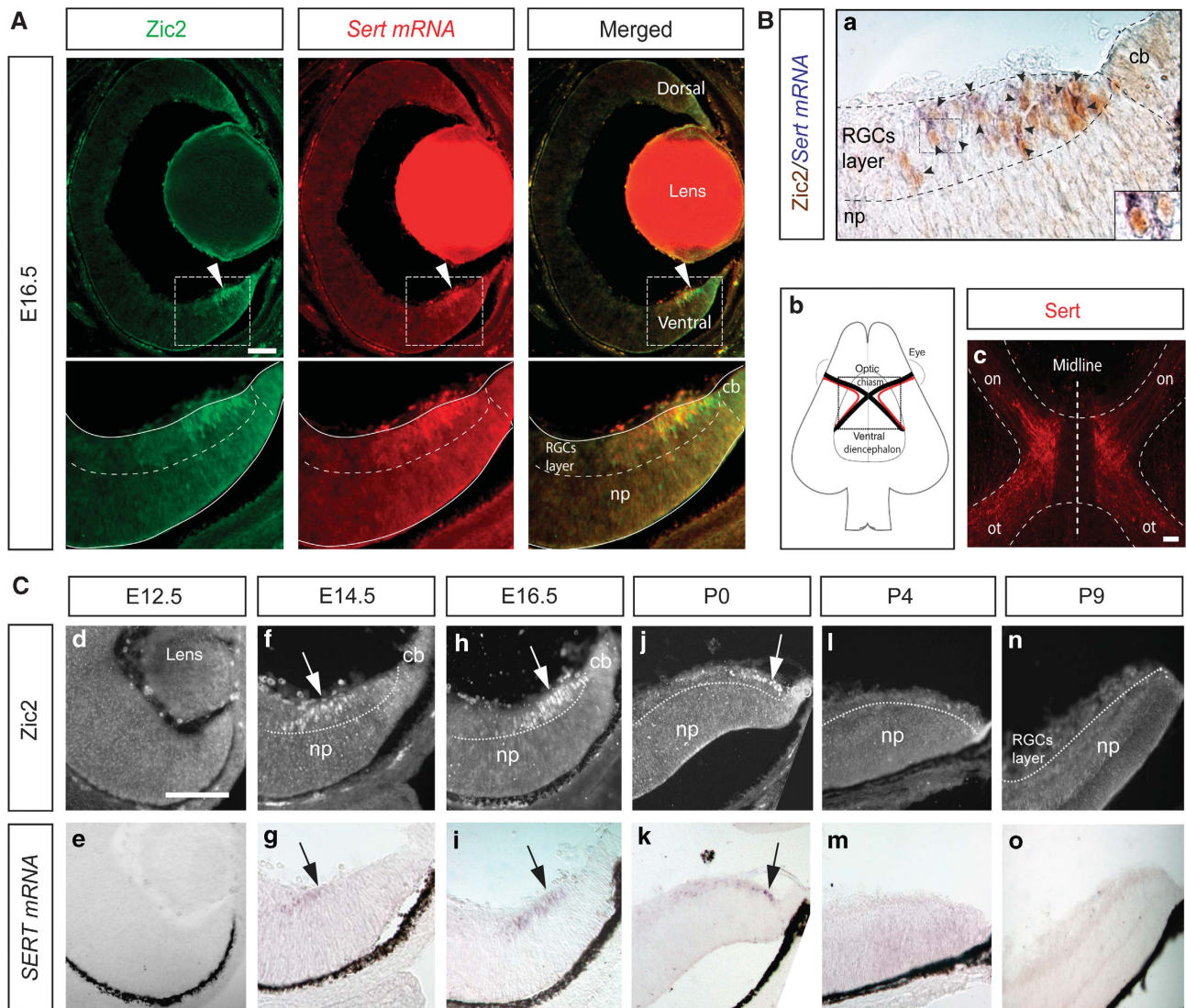


Figure 2 Spatio-temporal co-localization of Zic2 and Sert in iRGCs. (A) Fluorescent immunostaining against Zic2 (green) combined with *in situ* hybridization for Sert (red) performed in a coronal section from an E16.5 mouse retina shows that Zic2 and Sert are expressed in the peripheral ventrotemporal retina. Below each image, higher magnifications of the corresponding-squared areas are shown. (B, a) Colorimetric immunostaining against Zic2 combined with *in situ* hybridization for Sert demonstrate that cells expressing *Sert mRNA* (purple) are Zic2-positive neurons (brown). Black arrowheads highlight cells that are double positive for Zic2 and *Sert mRNA*. The right corner contains a high magnification of the squared area. np, neural progenitors; cb, ciliary body. Scale bar: 100 μ m. (B, b) Scheme showing a ventral view of the diencephalon that includes the optic chiasm area. Black lines represent contralateral axons and red lines represent ipsilateral axons. (B, c) The picture shows an immunohistochemistry against Sert (red) performed in a semi-intact preparation that contains the optic chiasm region. Sert expression is localized in ipsilateral axons, whereas axons crossing the midline are Sert negative. on, optic nerve; ot, optic tract. Scale bar: 100 μ m. (C) Top panels show immunostaining against Zic2 (white arrows) in VT retinal sections from E12.5 (d, e), E14.5 (f, g), E16.5 (h, i), P0 (j, k), P4 (l, m) and P9 (n, o) mice. Bottom panels show *in situ* hybridization against *Sert mRNA* (black arrows) in the same sections. The expression of both genes peaks at E16.5 and it is completely downregulated by P4. RGCs, retinal ganglion cells; cb, ciliary body; np, neural progenitors. Scale bar: 100 μ m.

qRT-PCR. Central retinas co-electroporated with pCAG-Zic2 and pCAG-EGFP (Zic2/EGFP) and collected 24 or 72 h after electroporation showed a significant increase of 2.0-fold and 2.5-fold, respectively, in the levels of *Sert mRNA* compared with samples electroporated with pCAG-EGFP alone (Figure 3B). Together, these results indicate that, *in vivo*, Zic2 is necessary and sufficient to induce Sert expression in the mouse retina.

Zic2 directly activates Sert transcription

To determine if Sert is a direct transcriptional target of Zic2, we investigated whether this transcription factor activates Sert regulatory sequences. In order to find common

mechanisms for the regulation of Sert expression conserved through evolution, we used the Vista browser to align sequences upstream of the 5'UTR of the Sert gene from six different mammalian species (human, monkey, dog, horse, rat and mouse) (Figure 4A). We found a 130-bp fragment immediately upstream of the transcriptional start site (TSS) (Bengel *et al*, 1997) that was highly conserved. Interestingly, this fragment contained fundamental information to drive transcription, including a TATA-like motif, a cyclic-AMP response element motif, a CG-rich sequence and several potential binding sites for transcription factors including Gli (Figure 4A).

To study the potential capacity of Zic2 to activate Sert transcription, the 130-bp conserved sequence (putative Sert

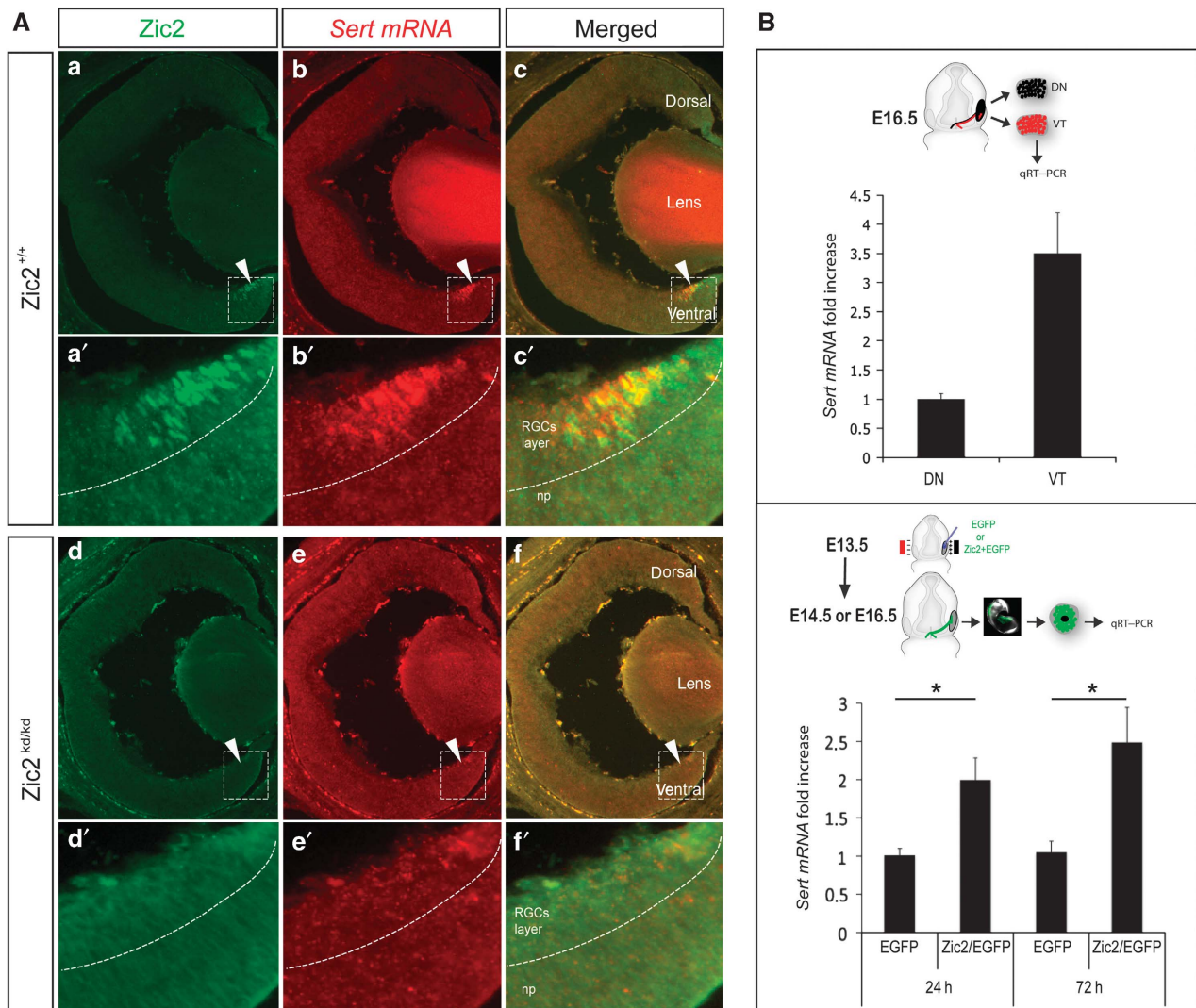


Figure 3 *Zic2* is necessary and sufficient for the expression of *Sert* in the retina. (A) The images show coronal retinal sections from WT (a–c), and homozygous *Zic2^{kd/kd}* (d–f) E16.5 littermate embryos. Immunostaining against *Zic2* in these sections shows that it is expressed in the VT retina in *Zic2^{+/+}* and disappears in *Zic2^{kd/kd}* embryos. *In situ* hybridization to *Sert* (red) in the same retinal sections demonstrates that *Sert* is highly downregulated in the absence of *Zic2*. Scale bars: 100 μ m. (B) The top panel shows quantitative RT–PCR analysis performed on segments from dorsonasal (DN) or VT E16.5 WT retinas to detect *Sert* mRNA. *Sert* mRNA levels were three-fold higher in the VT than in the DN retina. The bottom panel shows quantitative RT–PCR comparisons for *Sert* mRNA performed on central retinas of embryos electroporated at E13.5 with CAG-EGFP or with CAG-*Zic2*/CAG-EGFP plasmids and dissected out 24 or 72 h after electroporation. At least three retinas for each condition were pooled per experiment. The average of three and five different experiments is shown for 24 and 72 h, respectively. Error bars indicate \pm s.e.m. (* P <0.05, Student’s unpaired *t*-test).

promoter region) was amplified by PCR, cloned into a luciferase reporter plasmid (pGL3-basic), and used for luciferase assays in 293HEK cells. The transfection of the empty pGL3-basic plasmid, plus the empty pCAG plasmid or a mammalian expression vector containing the full-length *Zic2* sequence (pCAG-*Zic2*), all resulted in basal luciferase activity. When pGL3 bearing the putative *sert* promoter region (pGL3-*Sert* promoter) was co-transfected with an empty pCAG plasmid, luciferase activity above the basal level was detected, confirming the previously reported transcriptional activity of this region (Heils *et al*, 1998). When pCAG-*Zic2* was transfected in combination with the pGL3-*Sert* promoter into 293HEK cells, the luciferase levels increased more than seven-fold compared with the levels from the pGL3-*Sert* promoter and the empty pCAG plasmid. This demonstrates that *Zic2* is able to bind to this

130 bp-basic *sert* promoter region and activate transcription (Figure 4B). We also tested the activity of the TATA-like domain together with the GC-rich domain. However, this sequence alone was not able to augment basal luciferase activity in either the presence or absence of *Zic2*. Thus, the rest of the elements in the 130-bp fragment located upstream of the *sert* TSS are essential to induce transcription (data not shown).

Although the molecular mechanism of *Zic* gene-regulatory function is poorly understood, with few available *in vivo* validated DNA-binding sequences, *Zic* genes are known to bind to Gli sites (Mizugishi *et al*, 2001). Thus, in order to further characterize the domain where *Zic2* is binding inside the conserved 130 bp *sert* promoter, we mutated the Gli-binding site (Gli-BS). This resulted in a significant reduction in the activation of the *sert* promoter (Figure 4B). However, the basal activity of the promoter also

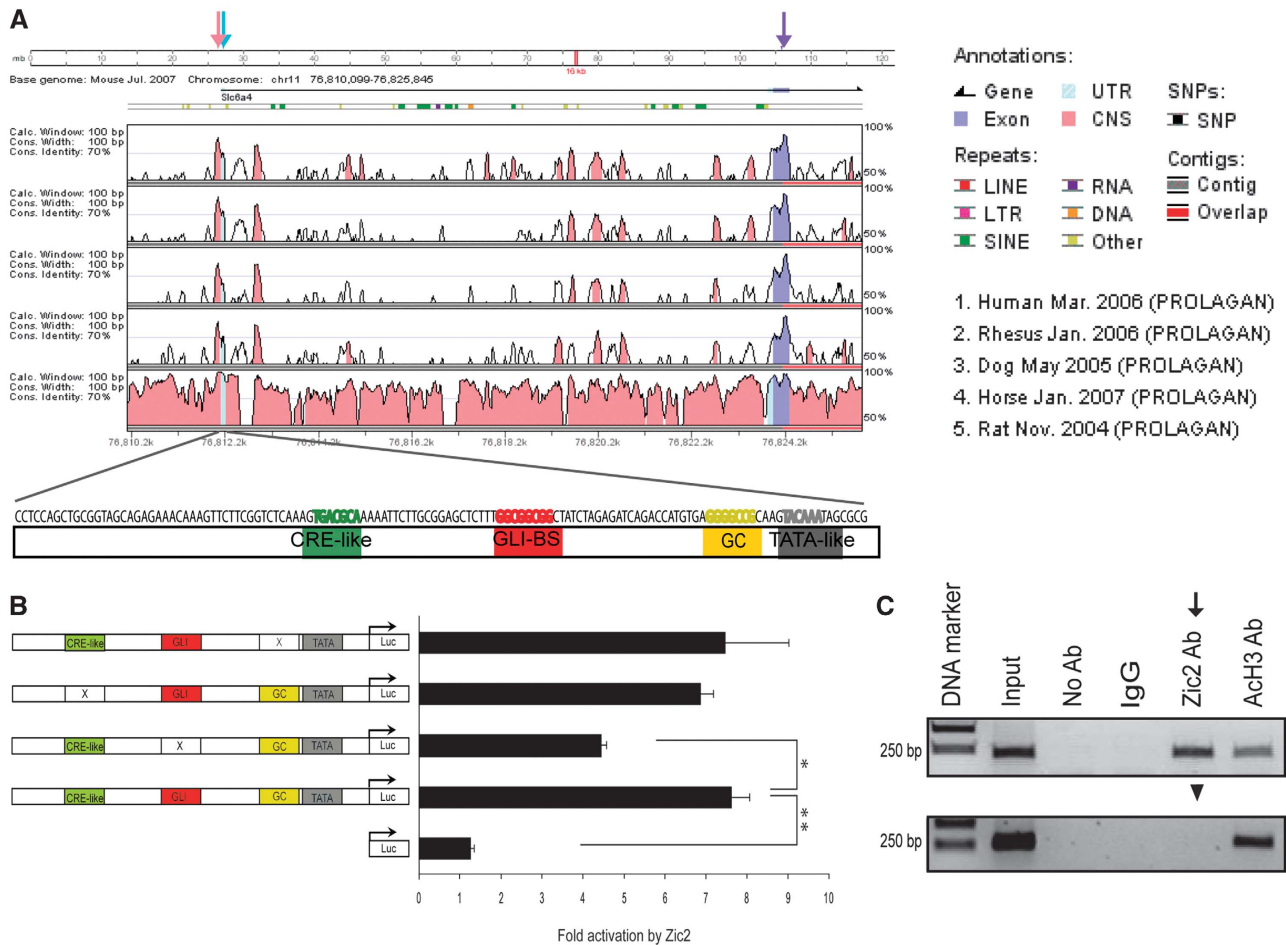


Figure 4 Zic2 directly regulates Sert expression. **(A)** VISTA view of the occurrence of conserved sequence domains upstream of the first *sert* exon (purple arrow). Light blue arrow indicates the consensus transcription start site of *sert* (TSS). Shown from top to bottom are human versus mouse (H/M), monkey versus mouse (M/M), dog versus mouse (D/M), horse versus mouse (H/M) and rat versus mouse (R/M) sequences. The coloured peaks (purple: coding, blue: UTR, pink: conserved non-coding regions) indicate regions of at least 100 bp, with a conservation score of at least 75%. The pink arrow indicates a highly conserved peak of 130 bp upstream of the TSS that has been proposed as the basal Sert promoter sequence. The 130 bp mouse sequence of the conserved Sert promoter, including putative binding sites (in different colours) for the indicated transcription factors is graphically represented below the VISTA comparison. **(B)** Luciferase assays to evaluate the transcriptional activity of Zic2 on the 130 bp Sert promoter region. After transfection of pCAG-Zic2 in 293HEK cells together with luciferase vectors containing the 130-bp Sert promoter region, Zic2 increases the basal transcriptional activity of the 130-bp conserved Sert promoter more than seven-fold compared with the controls. A mutation in the Gli-binding sequence significantly reduces this induction. By contrast, mutations in the CRE-like motif or the GC-rich domain of the *sert* promoter had no effects on the induction by Zic2. The values represent means \pm s.e.m. of at least four triplicates, except for pGL3-GC with two triplicates ($*P < 0.01$, Student's unpaired *t*-test). **(C)** ChIP assays demonstrate that Zic2 binds to the basal promoter region of Sert in the embryonic E16.5 VT retina *in vivo*. In the upper panel, primers to amplify the 130-bp Sert basal promoter were used, whereas in the bottom panel, control primers to amplify a 5'upstream non-conserved sequence were used. Zic2 binds to the Sert basal promoter (black arrow) but not to the control sequence (black arrowhead). Anti-Ach3 antibodies were used as positive controls and non-specific rabbit serum as negative control (IgGs).

decreased. To investigate if this reduction in basal activity could account for the decreased activation by Zic2 we created two independent mutations in the *sert* promoter that also produced significant reductions in basal activity. However, neither of these mutations changed the ability of Zic2 to activate the *sert* promoter (Figure 4B). This suggests that Zic2 interacts specifically with the Gli-BS.

Given that in 293HEK cells Zic2 increases the luciferase activity driven by the conserved region of the *sert* promoter, we determined whether Zic2 binds to this Sert regulatory sequence in the retina *in vivo*. Chromatin immunoprecipitation (ChIP) assays were carried out using anti-Zic2-specific antibodies and chromatin from VT retinal segments of E16.5 WT mouse embryos. Primers flanking the 130-bp *sert* promoter region were used for PCR amplification. The ChIP

assays confirmed the specific binding of Zic2 to the 130-bp sequence located immediately upstream of the *sert* TSS. No PCR product was detected in the negative control using primers designed to an adjacent region upstream of the conserved promoter region (1 Kb upstream of the *sert* TSS). As a positive control, an anti-Acetyl-Histone3 (ACh3) antibody was used (Figure 4C). These results demonstrate that Zic2 is able to regulate the expression of Sert in iRGCs *in vivo* by direct binding to its promoter region.

RGCs that ectopically express Zic2 project in the contralateral domain of visual targets

The function of the serotonin signalling pathway, and more specifically Sert, in visual system development had been characterized previously. Mice that lack Sert or that have

been treated with Sert inhibitors exhibit defects in the eye-specific refinement process of ipsilateral RGC axons (Upton *et al*, 1999; Salichon *et al*, 2001), an alteration that we have also confirmed (Supplementary Figure S2). On the basis of these findings and given that *Zic2* controls *Sert* expression in iRGCs, we decided to examine whether *Zic2* has a function in refinement at the visual targets.

Zic2^{kd/kd} mice die at embryonic stages and a conditional approach to remove *Zic2* specifically in the eye and analyse the projection pattern of iRGCs is not feasible because the lack of *Zic2* in the retina causes the elimination of the ipsilateral projection (Herrera *et al*, 2003). Taking advantage of our previous observation that ectopic expression of *Zic2* in the central retina induces the expression of *Sert* (Figure 3B), we took a gain-of-function approach instead. Plasmids bearing EGFP, as a control, or *Zic2* plus EGFP (*Zic2*/EGFP)-coding sequences were expressed ectopically in RGCs from the centre of the retina by *in utero* electroporation at E13.5. We analysed the projection pattern of these targeted axons in both the dLGN and SC in P15 mice when the axonal refinement/segregation process is complete (Figure 5). In order to label the endogenous ipsilateral and contralateral projections at the visual targets, electroporated mice were monocularly

injected with an axonal tracer (Cholera toxin subunit B (CTB)-Alexa-Fluor 594).

Axons expressing EGFP alone were found projecting inside the territory occupied normally by contralateral axons in both dLGN and SC (Figure 5). As reported previously, ectopic expression of *Zic2*/EGFP in the centre of the retina caused ~40–45% of targeted RGCs to switch laterality and project ipsilaterally (García-Frigola *et al*, 2008; Petros *et al*, 2009). The analysis of these ectopic *Zic2*-positive axons revealed that they were able to find their way to the ipsilateral dLGN and SC in spite of being in the wrong hemisphere. Furthermore, although their axonal arborization was deficient and neurite processes were poorly elaborated, they were all found in the territory normally occupied by contralateral axons (Figure 5). This demonstrates that, although their laterality at the chiasm is altered, central RGCs expressing ectopically *Zic2* still project into the contralateral eye-specific domain as it corresponds to their ‘central-contralateral’ position in the retina.

RGCs that ectopically express Zic2 do not refine properly in the SC

Although RGCs expressing *Zic2* ectopically projected into contralateral domains, their projection phenotype was

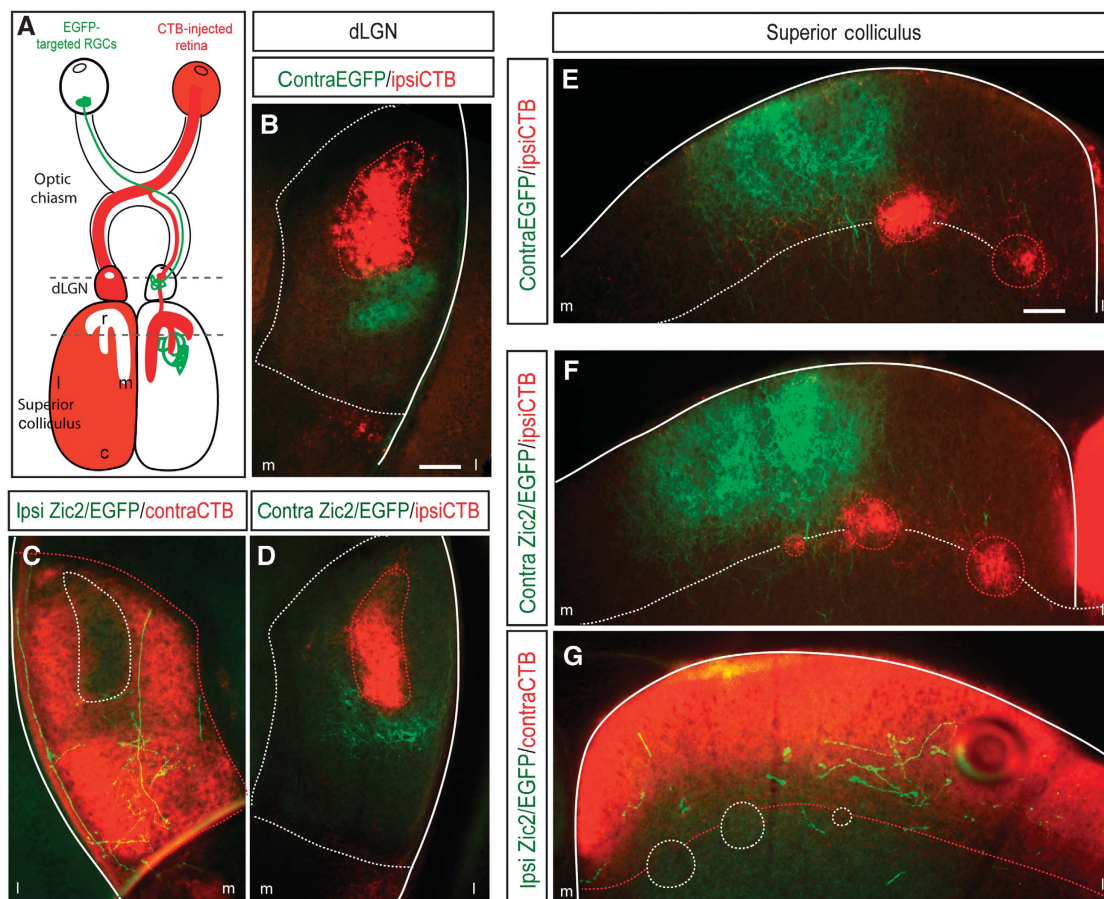


Figure 5 Axons that ectopically express *Zic2* project into the contralateral-specific domain in the visual targets. (A) Summary of the experimental approach used to visualize retinal axons at the dLGN and SC. Plasmids bearing EGFP or *Zic2*/EGFP were introduced in central RGCs by *in utero* electroporation at E13.5. At P14, electroporated mice were monocularly injected with the axonal tracer cholera toxin subunit B (CTB-Alexa594) and they were killed 1 day later. Dashed lines indicate the level of the sections. Representative coronal sections through the dLGN of P15 mice electroporated with EGFP (B) or with *Zic2*/EGFP (C, D) show that all targeted axons project into contralateral-specific domains. (E–G) Representative coronal sections through the SC of P15 mice electroporated with EGFP or with *Zic2*/EGFP show that all targeted axons project into contralateral-specific domains. Red-dashed lines outline the territory occupied by axons coming from the CTB-injected eye. White-dashed lines outline the territory occupied by axons coming from the non-injected eye. m, medial; l, lateral. Scale bars: 100 μm.

abnormal. To further investigate this issue, and as alterations in the serotonin pathway produces more evident phenotypes in the SC than in the dLGN, we studied the projection of targeted axons in the SC of electroporated animals. We first characterized the projection pattern of central RGCs during development. Brains of mice electroporated at E13.5 with EGFP alone were killed at three different time points, P0, P4 and P15, dissected out and sectioned sagittally to evaluate the rostrocaudal distribution of the targeted projections. At P0

and P4, EGFP-positive axons had reached the most caudal area of the colliculus. By P15, targeted axons had already refined and formed complex and elaborated arbors in the medial area of the colliculus contralateral to the electroporated eye (Figure 6). EGFP-positive axons were not found in the ipsilateral SC.

Next, we analysed the projections of Zic2/EGFP-electroporated axons. In this case, targeted axons were always found in both the contralateral and the ipsilateral side of the

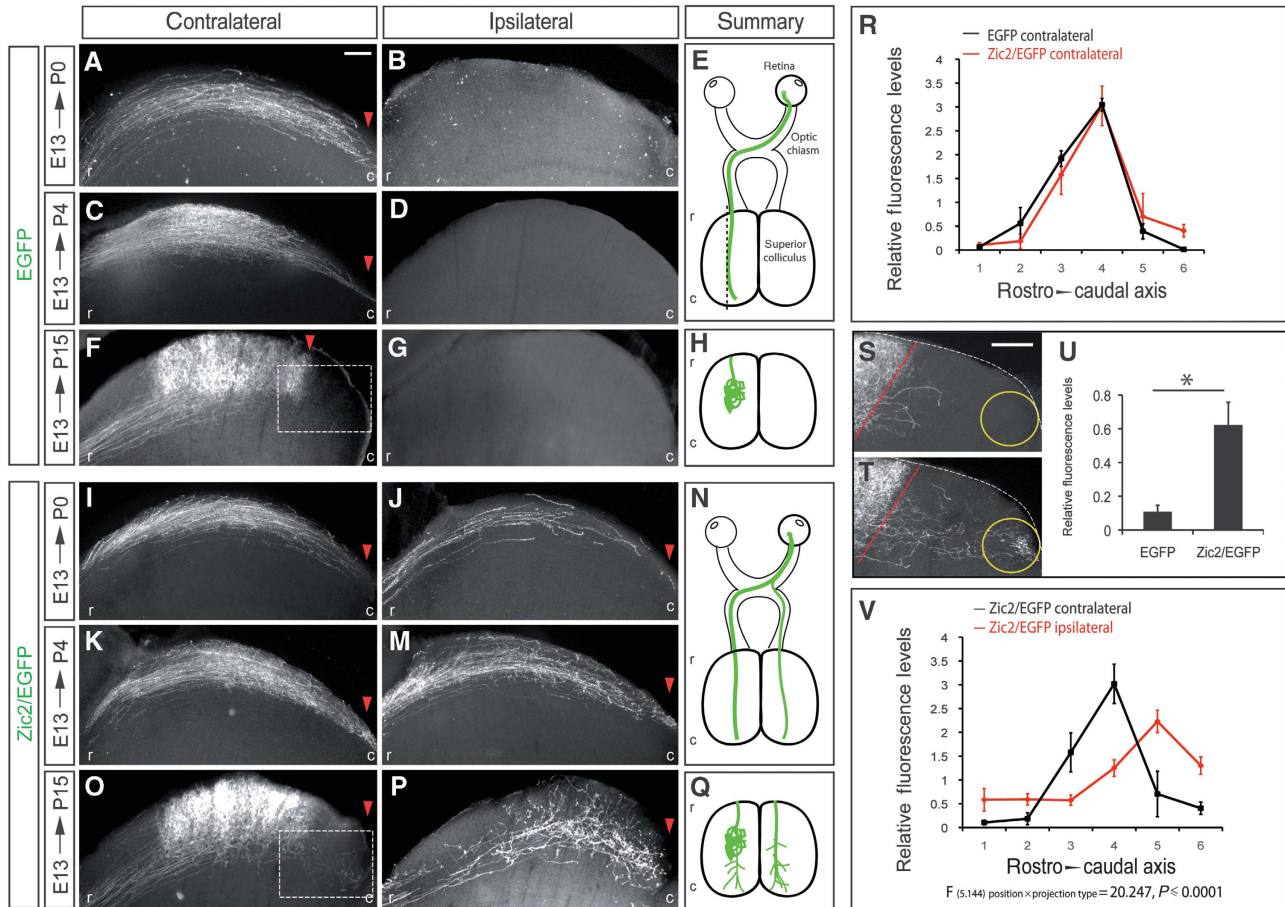


Figure 6 Axons that ectopically express Zic2 do not refine properly at the colliculus. (A–G) Pictures show representative sagittal sections of the SC from P0, P4 and P15 mice that were electroporated with plasmids bearing the coding sequence of EGFP in the central retina at E13.5. (A) In the hemisphere contralateral to the electroporated eye, EGFP-positive axons coming from the central retina reach the caudal region of the colliculus at P0. (C) Four days later, at P4, although a high proportion of axons were found in the caudal collicular region, many of them have started to refine and arborize into more central areas. (F) By P15, all axons have already refined and they can be found only in central areas of the SC. (B, D, G) Pictures show that EGFP-positive axons were not found in the ipsilateral side at any stage. (I–P) Pictures show representative sagittal sections of the SC from P0, P4 and P15 mice that were co-electroporated in the central retina at E13.5 with plasmids bearing the coding sequence of Zic2 and EGFP. (I, K) In the hemisphere contralateral to the electroporated eye, Zic2/EGFP-positive axons coming from the central retina reach the caudal region of the colliculus at P0 and P4. (O) By P15, many axons have already refined and they can be found in central areas of the SC. In this case, in contrast to the EGFP control, some targeted axons were detected in the caudal areas. (J, M, P) In the ipsilateral side of Zic2/EGFP-electroporated mice, targeted axons were found in the caudal colliculus at all the stages, including P15. Red arrowheads highlight the most caudal position where targeted axons were visualized. (E, N) Schematic representations of the projection phenotypes along the visual pathway summarize the results obtained in mice electroporated at E13.5 and analysed at P0 and P4. (H, Q) Schematic representation of the projection phenotype in the SC of animals electroporated with EGFP or Zic2/EGFP at E13.5 and analysed at P15. (R) Quantitative comparison of fluorescence measurements in the contralateral colliculus of P15 mice electroporated with EGFP or with Zic2/EGFP at E13.5. Despite no overall significant differences were found comparing the axonal distribution in the sections of EGFP and Zic2/EGFP-electroporated mice, it is important to note the increase in the fluorescence values of the Zic2/EGFP in the most caudal point of the SC. (S, T) High magnification pictures of the caudal-squared areas in (F) and (O). The red-dashed lines delineate the caudal limit of the correct TZ according to the central location of the targeted RGCs in the retina. (U) Quantification of the levels of fluorescence in the caudal region of collicular sagittal sections (yellow circle) from P15 mice shows a significant increase in the amount of fluorescence in Zic2/EGFP-electroporated mice compared with the controls. Data obtained from six animals and three sections from each animal for each condition (* $P \leq 0.05$, Student's unpaired *t*-test). (V) Quantitative analysis of fluorescence measurements in sagittal sections comparing contralateral versus ipsilateral P15 colliculus electroporated with Zic2/EGFP show that the distribution of the projections on each side is significantly different. Error bars indicate \pm s.e.m. Statistical analysis was performed using a two-way ANOVA ($F_{(5,144)} \text{ position} \times \text{projection type} = 20.247, P \leq 0.0001$). Data obtained from four animals and three sections from each animal for each condition. r, rostral; c, caudal. Scale bars: 100 μm .

colliculus. At P0 and P4, Zic2/EGFP axons had reached the caudal areas of the SC, similar to when only EGFP is electroporated. However, at P15, defects were seen in EGFP/Zic2-positive axons in both the ipsilateral and contralateral SC. In the ipsilateral SC, EGFP/Zic2 axons remained in caudal areas instead of in the central region appropriate to the location of their cell bodies in the retina. In addition, the terminal fields of these neurons were diffuse, showing a deficient elaboration of axon arbors (Figure 6). In the contralateral SC, most EGFP/Zic2-electroporated axons projected properly into their correct termination zone in the medial SC. However, we found consistently that a small proportion were located ectopically in caudal areas (Figure 6R). As we co-electroporated two plasmids (pCAG-Zic2 and pCAG-EGFP), it is likely that axons correctly projecting and arborizing in the medial areas of the colliculus are those that express EGFP but do not co-express Zic2 or express it at low levels. Conversely, the axons that misproject into caudal areas are likely Zic2-positive fibres that had already passed the midline when ectopic Zic2 expression was initiated. In order to quantify the extent of this abnormal projection in the contralateral SC, we performed fluorescence quantifications on the caudal collicular area of animals electroporated with Zic2/EGFP and found a significant increase in fluorescence in this area compared with controls electroporated only with EGFP (Figure 6S–U). This projection of Zic2-transfected axons beyond their topographically correct TZ resembles the projection errors caused by pharmacological or genetic alteration of serotonin levels during development (Bastos *et al*, 1999; Upton *et al*, 2002; Ravary *et al*, 2003; Gonzalez *et al*, 2008).

Zic2-positive but not Zic2-negative RGC axons respond to pharmacological blockage of Sert

Next, we investigated whether the lack-of-refinement phenotype observed in the axons ectopically expressing Zic2 is due to the misexpression of Sert. In order to test this hypothesis, we electroporated E13.5 embryos in the central retina and waited until the mice were born. Then, we administered a daily dose of fluoxetine, a well-known inhibitor of Sert (Wong *et al*, 1974, 1995), until they were analysed at P15. Fluoxetine treatment induced a significant change in the TZs of RGC axons electroporated with Zic2, producing a medial shift of the projections back to their topographically correct location (Figure 7A–C). In general, we also observed that after fluoxetine treatment, Zic2-positive fibres showed a more exuberant elaboration of axon arbors compared with Zic2-positive saline-treated fibres.

In the contralateral SC of P15 mice electroporated with Zic2/EGFP, we focused our analysis in the caudal collicular areas (Figure 7D and E) that contain the axons with a defect in refinement. We found that in fluoxetine-treated mice, the extent of aberrant axon projections within the caudal collicular area was reduced significantly compared with saline-treated animals (Figure 7D–F). We cannot rule out the possibility that Zic2 controls other molecules that also participate in refinement processes at the SC. Nevertheless, the partial rescue of the Zic2 misexpression phenotype by blocking Sert demonstrates clearly that Zic2 upregulates Sert, which then inhibits the proper refinement and arborization of retinal axons at the colliculus.

Previous reports have examined how alterations in serotonin levels affect the refinement of ipsilateral RGCs axons at

the SC (Bastos *et al*, 1999; Upton *et al*, 2002; Gonzalez *et al*, 2008). However, the phenotype of contralateral RGC axons after changing serotonin concentrations has not been evaluated, likely because the analysis of contralateral axons is technically more challenging. To investigate this issue, we electroporated EGFP in central RGCs at E13.5 followed by treatment with fluoxetine or saline as described above. EGFP-targeted axons project to their correct TZ, the medial portion of the colliculus and the degree of arborization was very similar in fluoxetine and saline-treated animals (Figure 7G–I). This demonstrates that inhibition of Sert does not affect the refinement of cRGCs. Together with previous results, these findings demonstrate that Zic2 controls specifically the refinement of ipsilateral but not contralateral axons in the primary visual targets by controlling directly the expression of Sert.

Zic2 modulates refinement at the SC independently of controlling laterality at the midline

As the stronger refinement phenotype in Zic2-electroporated animals was found in the ipsilateral SCs, we wanted to rule out the possibility that switching laterality at the midline affects axonal refinement at the targets. To address this, we expressed ectopically EphB1 in the central region of the retina and analysed postnatally the retinocollicular projections. In agreement with previous reports, we found that ectopic expression of EphB1 resulted in 15–20% of the targeted axons projecting ipsilaterally (García-Frigola *et al*, 2008; Petros *et al*, 2009). However, we found that EphB1-electroporated axons on both the ipsilateral and contralateral SC formed TZs in the topographically correct location (Figure 8A). This demonstrates that a switch in axonal laterality does not determine the eye-specific territory, topographic projection pattern or refinement at the target. This result also suggests that contact of RGCs axons with midline cues does not generate a retrograde signal that modulates the projection patterns at the targets. We also found that Sert expression is independent of EphB1. In mice lacking EphB1, expression of Sert in the retina was maintained in a pattern indistinguishable from wild type (Figure 8B).

Next, we asked if Sert is required for guidance at the midline. In contrast to ectopic expression of Zic2 or EphB1, we found that electroporation of Sert (pCAG-Sert) in central RGCs did not affect guidance at the midline (Figure 8D). In agreement with previous reports (Upton *et al*, 2002), we also found that Sert-deficient mice did not exhibit any alteration in the number of ipsilateral RGC axons (Supplementary Figure S2). This indicates clearly that Sert does not have a function in controlling guidance at the midline. Together, these results demonstrate that axon guidance at the midline and refinement of ipsilateral axons in the SC are independent phenomena. Zic2 has a function in both processes by activating independently different effectors: EphB1 to control laterality and Sert to modulate refinement at the visual targets.

Discussion

In this study, we show that the transcription factor Zic2 has an important function in controlling eye-specific refinement in the SC by inducing the expression of Sert specifically in iRGCs. Together with previous results, this demonstrates that Zic2 determines the ipsilateral phenotype in the retinofugal

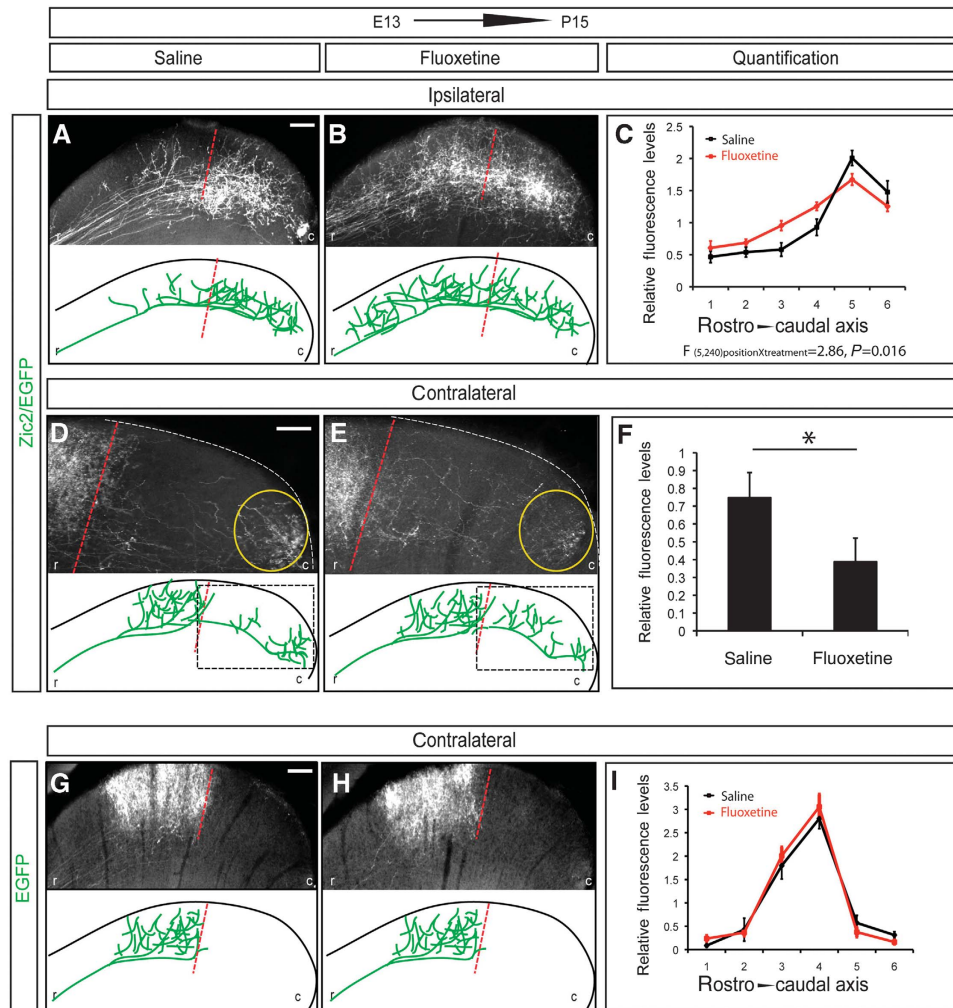


Figure 7 Zic2-positive but not Zic2-negative axons respond to fluoxetine treatment. The pictures show representative sagittal sections of the SC from P15 mice that were electroporated at E13.5 in central retina and then treated with saline or fluoxetine from P0 to P15. To summarize the results, schematic representations of collicular sections are shown below each image. The red-dashed lines delineate the caudal limit of the correct TZ according to the central location of the targeted RGCs in the retina. **(A, B)** In the ipsilateral SC of animals electroporated with Zic2/EGFP, axons projected to more rostral areas in fluoxetine-treated than in saline-treated animals. **(C)** Quantitative analysis of fluorescence measurements in sagittal sections of colliculus electroporated with Zic2/EGFP treated with saline versus fluoxetine shows a significant displacement of the projection to more rostral positions after fluoxetine treatment ($F(5,240)_{\text{position} \times \text{treatment}} = 2.86, P = 0.016$). Data obtained from five animals and four equivalent sections from each animal for each condition. **(D, E)** High-magnification pictures of the caudal portion of the contralateral SC (squared area) of mice electroporated with Zic2/EGFP show that axons treated with fluoxetine project to more rostral areas than those treated with saline. **(F)** Quantification of the levels of fluorescence in the caudal region of collicular sagittal sections (yellow circle) shows a significant decrease in the amount of fluorescence in the fluoxetine-treated animals compared with the saline-treated animals ($*P \leq 0.001$, Student's unpaired *t*-test). Data were obtained from six animals and three sections from each animal for each condition. **(G, H)** In the contralateral SC of animals electroporated with EGFP, axons project in the medial region in both saline and fluoxetine-treated mice. As EGFP axons did not project into the ipsilateral side, the ipsilateral colliculi are not shown. **(I)** No significant differences were found after quantitative analysis of fluorescence measurements in sections of SCs from EGFP-electroporated mice treated with saline versus fluoxetine. Data were obtained from three animals and three equivalent sections from each animal per treatment. Error bars indicate \pm s.e.m. Statistical analysis was performed using a two-way ANOVA. r, rostral; c, caudal. Scale bars: 100 μ m.

pathway by regulating the transcription of at least two downstream effectors, EphB1 and Sert, which act sequentially at different steps of the maturation process in the visual pathway.

Zic2 controls the transient expression of Sert during development

Several days after the generation of the raphe neurons, serotonin accumulation can be detected in several classes of thalamic, cortical, hypothalamic and retinal neurons. These neurons do not express tryptophan hydroxylase (Tph) or dopa decarboxylase (Aadc), which are required for

serotonin synthesis, or the catabolic enzymes monoamine oxidase A and B. The presence of serotonin in these neurons is explained by the transient expression of Sert that reuptakes serotonin from the extracellular space (Gaspar *et al*, 2003). The transcriptional network controlling the levels of serotonin in the raphe nuclei has been intensely studied. The transcription factor Pet1 is expressed in serotonergic neurons and directly activates the transcription of genes that are involved in the synthesis (Tph and Aadc) and uptake (Sert) of serotonin. However, not much is known about the regulation of the transient Sert expression in non-aminergic neurons. The transcriptional mechanisms controlling serotonin

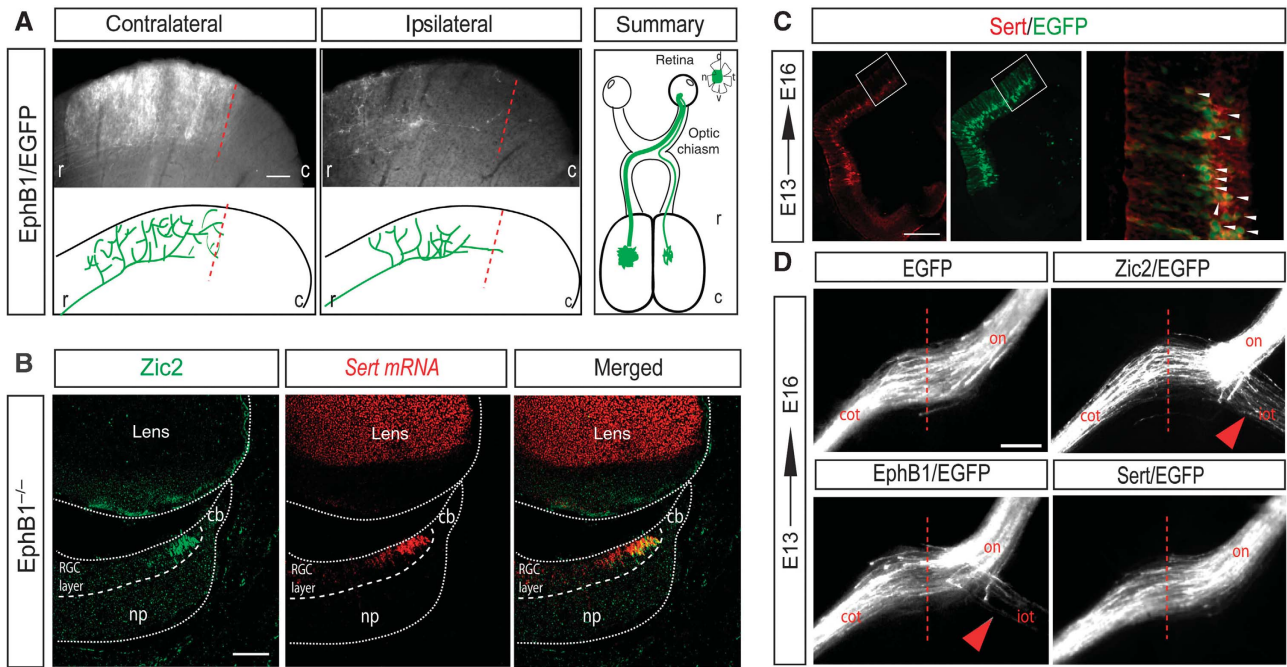


Figure 8 *Zic2* controls refinement at the SC independently of controlling axon guidance at the midline. (A) Pictures show representative sections of the SC from P15 mice electroporated at E13.5 with CAG-EphB1 plasmids. Axons ectopically expressing EphB1/EGFP project to the medial region in both, the contralateral and the ipsilateral SC. Schematic representations of collicular sections are shown below each image. Dashed lines delineate the caudal limit of the correct TZ according to the location of targeted RGCs in the retina. In the right panel, the projection phenotypes are summarized. Sections from four different embryos electroporated with EphB1/EGFP were analysed and all of them showed similar phenotypes at the colliculus. r, rostral; c, caudal; (B) Coronal section from an E16.5 *EphB1*^{-/-} VT retina, in which an immunostaining against *Zic2* (green) was combined with *in situ* hybridization to *Sert* (red) shows that expression of *Sert* is normal in the absence of EphB1. np, neural progenitors; cb, ciliary body. Scale bars: 100 μ m. (C) Immunostaining against *Sert* (red) in sections from E16.5 embryos electroporated with *Sert/EGFP* (green) at E13.5 confirms ectopic expression of *Sert* in the targeted area. (D) The picture shows the optic chiasm region of E16.5 embryos electroporated with different plasmids at E13.5. In embryos electroporated with EGFP alone or with *Sert/EGFP*, all targeted axons cross the midline, contrasting with *Zic2/EGFP* or EphB1/EGFP-electroporated embryos that show ipsilateral and contralateral axons at the optic chiasm. Red arrows point to the ectopic ipsilateral projection. Red-dashed lines mark the midline. on, optic nerve; iot, ipsilateral optic tract; cot, contralateral optic tract. Scale bar: 500 μ m.

signalling in these neurons probably differ from those uncovered in the raphe nuclei, as none of the genes that regulate the serotonin phenotype in the raphe have been found in areas that transiently express *Sert*. The results presented here support this hypothesis and point to *Zic2* as the first transcription factor that regulates *Sert* expression and serotonin homeostasis in non-aminergic neurons during development.

***Sert* as a modulator of activity-dependent refinement**

We demonstrate here that *Zic2* induces directly the transcription of *Sert* in iRGCs. *Sert* is known to adjust the extracellular concentration of serotonin (Wong *et al*, 1974; Jennings *et al*, 2006). Serotonin signalling has a critical function in axonal refinement processes in several systems and animal models. Genetically modified mice lacking monoamine oxidase A, an enzyme that breaks down serotonin, exhibit severe disruptions in the barrels domains of the primary somatosensory cortex (Rebsam *et al*, 2002) as well as in eye-specific segregation in the dLGN and SC (Upton *et al*, 1999). In rodents, increased levels of serotonin prevent the segregation of retinocollicular axon terminals (Upton *et al*, 2002) and decreasing serotonin levels by parachlorophenalanine treatment or by neonatal tryptophan restriction in the diet, also affect retinofugal fibre refinement (Upton *et al*, 1999; Gonzalez *et al*, 2008). Similarly, pharmacological blockade or genetic removal of *Sert* perturbs eye-specific refinement of retinal

axons at the visual targets (Bastos *et al*, 1999) or barrels formation in the cortex (Xu *et al*, 2004).

As cAMP signalling is essential for the segregation of eye-specific inputs (Stellwagen *et al*, 1999; Pham *et al*, 2001; Ravary *et al*, 2003) it is likely that, as in other systems, serotonin signalling acts in the visual system by affecting cAMP levels. Serotonin receptors (5HT_{1B}) are localized in all RGCs axon terminals (Salichon *et al*, 2001). The 5HT_{1B} receptor is negatively coupled to the adenylate cyclase 1 (AC1) through G-proteins of the G α i subtype (Lin *et al*, 2002). AC1 has an important function in the refinement of the ipsilateral retinal projection in both the LGN and the SC, acting presynaptically in RGCs to modulate the reshaping of axon terminal arbors in the retinofugal projections and not affecting axon guidance in the travelling of retinal fibres to the targets (Ravary *et al*, 2003; Plas *et al*, 2004; Nicol *et al*, 2006, 2007). In cRGCs, the activation of the 5HT_{1B} receptor would inhibit cAMP production in the axon terminals. However, retinal axons that express adequate levels of *Sert* can internalize extracellular serotonin and relieve 5HT_{1B}-mediated inhibition, allowing the production of cAMP and promoting the refinement process (Supplementary Figure S3). Supporting this theory, mice lacking another component of the machinery, the 5HT_{1B} receptor, also show defects in eye-specific segregation in the LGN and SC (Upton *et al*, 1999).

Our data confirm previous reports showing that either, increasing or decreasing the levels of extracellular serotonin affect axon refinement in several sensory systems (Upton *et al.*, 1999, 2002; Xu *et al.*, 2004; Rebsam *et al.*, 2005; Gonzalez *et al.*, 2008). Sert null mice that have accumulated serotonin extracellularly show a 'lack-of-refinement' phenotype and mice that ectopically express Sert (induced by Zic2) exhibit similar alterations in the refinement process. Interestingly, it has been reported that rather than absolute cAMP levels, the appropriate balance of cAMP production and degradation is essential for retinal axon refinement (Nicol *et al.*, 2007). It is thereby likely that alterations, positive or negative, in the levels of serotonin disturb the production of cAMP oscillations preventing axonal refinement of ipsilateral axons.

Eye-specific layering at the targets: dependent or independent of laterality at the midline?

A number of observations indicate that axon laterality at the midline and the establishment of projection patterns and eye-specific segregation at the visual targets are independent events. The *Robo* and *Comm* mutants in *Drosophila* (Karlstrom *et al.*, 1996), the *astray* mutants in zebrafish (Wolf and Chiba, 2000), the Siamese and albino cats (Guillery, 1969; Creel *et al.*, 1982; Kliot and Shatz, 1985), and the achiasmatic sheepdogs (Williams *et al.*, 1994) show normal projection patterns at the final targets despite the fact that they all have alterations in the ipsi/contra ratio. In agreement with these observations, when we ectopically expressed EphB1 to force some cRGCs axons to switch laterality at the midline, they projected correctly in the topographic collicular area corresponding to their retinotopic position, a phenomenon similar to the situation previously described for the dLGN (Rebsam *et al.*, 2009). Our data confirm that divergence at the midline and determination of the projection phenotype at the targets are independent events. However, our findings also demonstrate that these processes are not unrelated because both require the action of a common transcription factor, Zic2.

In addition, in EphB1 null mice around 60% of the axons from the VT retina change laterality and are misrouted to the contralateral LGN (Williams *et al.*, 2003). Despite the change in laterality, these misrouted axons target in the topographic area that corresponds to the ipsilateral domain but in the contralateral side and segregate perfectly from the real contralateral axons, forming a patch that never mingle with the endogenous contralateral projections (Rebsam *et al.*, 2009). We have observed that the levels of Sert in the VT region of EphB1^{-/-} mice are normal, which indicates that these misrouted axons still express endogenous levels of Sert and argues for a function of this transporter in the segregation of VT axons even when they project in the wrong hemisphere.

Zic2, the first transcription factor involved in the establishment of RGC axonal refinement

We have shown that ectopic expression of Zic2 in central retina induces axons to project to mediocaudal areas of the SC. We have excluded the possibility that this phenotype is caused by a change in laterality. An alternative explanation to this finding is that Zic2 regulates some additional molecules involved in targeting at the colliculus. However, this is unlikely because ipsilateral axons, which naturally express Zic2, do not project caudally but rostrally. It seems more

plausible that ectopic expression of Zic2 in central retina affects the refinement process of these neurons because the relative levels of serotonin they sense are not perfectly balanced. Axons from the central retina first overshoot their TZs to innervate caudal positions of the SC to then retract and project in central positions (Simon and O'Leary, 1992). The ectopic expression of Zic2 in cRGCs leads to a lack-of-refinement phenotype of their axons, a defect that is partially reverted after application of fluoxetine indicating, at least in part, this phenotype is caused by induction of Sert.

It is not clear whether refinement and segregation are independent processes but changes in serotonin levels affect both. The cRGCs that are neighbouring the iRGCs arise from the VT retina and project to similar areas than ipsilateral fibres on the contralateral side but they eventually segregate from them. On the basis of this premise, and assuming that levels of EphA/ephrinAs and other axon guidance molecules determine the final projection pattern of all retinal axons, it is possible that iRGCs only differentiate from cRGCs in two aspects: (1) the decision of avoiding the midline and (2) the expression of molecules that permit the refinement/segregation process. Our results are on line with this idea because ectopic expression of Zic2 does not cause a change in the identity of central-contralateral cells to now project into the ipsilateral domain. According to this view, Zic2 would be a 'master-gene' that provides the necessary molecules to distinguish iRGCs from cRGC in these two stages of differentiation.

Overall, the results presented here link, for the first time, early molecular events in axon guidance with late activity-dependent refinement processes and points to Zic2 as an important regulator of different steps during the establishment of the visual circuitry in mammals.

Materials and methods

Animals

Mice from BDF1 (DBA2 x C57/B6) WT, Zic2^{+ /kd} (Nagai *et al.*, 2000), EphB1^{-/-} (Williams *et al.*, 2003) and Sert^{-/-} (Bengel *et al.*, 1998) strains were kept in a timed pregnancy breeding colony at the Instituto de Neurociencias (IN). Animal protocols were approved by the IN Animal Care and Use Committee.

Microarrays analyses

Total RNA was extracted from triplicate pools of 14–16 retinal VT segments from E16.5. WT and Zic2^{kd/kd} embryos. Samples were then processed as in Lopez de Armentia *et al.* (2007). The list of significantly changed probe sets shown in Figure 1 was obtained after filtering by signal intensities (20–100th percentile in the raw data), statistical significance ($P < 0.05$, unpaired *t*-test) and fold change (> 2.0) using GeneSpring GX software (Agilent Technologies, Santa Clara, CA).

In situ hybridization and immunohistochemistry

In situ hybridization was performed as in Schaeren-Wiemers and Gerfin-Moser (1993). To perform fluorescent reactions, TSA system (Perkin Elmer) was used following the manufacturer's instructions. To generate Sert probes, the following primers were used: ATCGTGGTCATCACTTGCATC-, GTTACACAGCATTCATGCCG-. Immunohistochemistry protocols were performed as in Herrera *et al.* (2003) and García-Frigola *et al.* (2008). Anti-Zic2 (Brown *et al.*, 2003) and anti-SERT antibodies (Blakely *et al.*, 1994) were used at 1:10 000 and 1:1000, respectively.

Quantitative RT-PCR

Retinas of E13.5 WT embryos were electroporated *in utero* with CAG-EGFP or CAG-Zic2 plasmids and qRT-PCR was performed as in García-Frigola *et al.* (2008).

Luciferase assays

A fragment of 130 bp was cloned into pGL3-Basic (Promega) (pGL3-Sert prom). Mutations in the CRE-like, GC-rich and Gli-BSSs were introduced by site-directed mutagenesis giving rise to the following sequence substitutions: GGCGGCG into GAATTCG; TGACGCA into GGATCCA and GGGGCGG into GAATTCG. Luciferase reporter plasmids carrying the corresponding mutations were named: pGL3-Gli mut, pGL3-CRE-like mut and pGL3-GC mut. The pCAG-Zic2 or the empty pCAG were co-expressed with the luciferase reporter plasmids. 293HEK cells plated in 24-well plates were co-transfected with 0.4 µg of a luciferase reporter plasmid (pGL3-Basic, pGL3-Sert prom, pGL3-Gli mut, pGL3-CRE-like mut or pGL3-GC mut), 10 ng of SV40-βgal and 0.4 µg of pCAG or pCAG-Zic2. After 24 h, cells were lysated and luciferase and β-galactosidase activities measured using Luciferase Reporter and Beta-Glo Assay Systems (Promega) following the manufacturer's guidelines. Each sample was assayed in triplicate and luciferase activities were normalized using β-galactosidase. The fold increase in luciferase activity was calculated as a ratio between the activity in the presence of Zic2 and the activity measured in the presence of the empty vector pCAG for each construct. Data were statistically analysed with SPSS using Student's unpaired *t*-test.

Chip assays

VT retinal quadrants from 2 litters of E16.5 embryos were dissected out and proteins cross-linked to DNA in a 1% formaldehyde solution for 20 min at room temperature. ChIP was carried out as described in the Upstate Biotechnology protocol. Zic2 was immunoprecipitated using anti-Zic2 antibodies (Brown *et al*, 2003) and control immunoprecipitations were performed using anti-acetylated-Histone3 (Sanchis-Segura *et al*, 2009), rabbit IgGs or no antibody. Primers used for amplification: Sert promoter: -CTGC TGTATGTGCAGGAATG-, -CGCGCTATTGTACTTGCGG-, Control -GCTGGTAGTTGTCTAGTCCC-, AGTCTCTGCTCCGTCTACTCC-.

In utero electroporation, fluoxetine treatment and CTB injections

Electroporation experiments were carried out in BDF1 (DBA2 × C57/B6) mice. Retinal *in utero* electroporation was performed as described in Garcia-Frigola *et al* (2007). For postnatal analysis in the LGN and SC, electroporated pups were killed and fixed at P15. Brains were sectioned for analysis and quantification of retinal projections in the targets. For fluoxetine treatment, a daily injection of fluoxetine (10 mg/kg, Sigma) or saline was administered subcutaneously from P1 to P4, and then intraperitoneally from P5 to P15. The corresponding retinas were removed and flat mounted to confirm electroporation in the central retina and to obtain a retinal electroporation ratio (retinal-electroporated area/total retinal area). CTB injections were performed at P14 as in Rebsam *et al* (2009).

References

Arce EA, Rhoades RW, Mooney RD (1995) Effects of neonatal and adult enucleation on the synaptic organization of the serotonergic projection to the superficial gray layer of the hamster's superior colliculus. *Brain Res Dev Brain Res* **90**: 168–173

Bastos EF, Marcelino JL, Amaral AR, Serfaty CA (1999) Fluoxetine-induced plasticity in the rodent visual system. *Brain Res* **824**: 28–35

Bengel D, Heils A, Petri S, Seemann M, Glatz K, Andrews A, Murphy DL, Lesch KP (1997) Gene structure and 5'-flanking regulatory region of the murine serotonin transporter. *Brain Res Mol Brain Res* **44**: 286–292

Bengel D, Murphy DL, Andrews AM, Wichems CH, Feltner D, Heils A, Mossner R, Westphal H, Lesch KP (1998) Altered brain serotonin homeostasis and locomotor insensitivity to 3, 4-methylenedioxymethamphetamine ('Ecstasy') in serotonin transporter-deficient mice. *Mol Pharmacol* **53**: 649–655

Blakely RD, De Felice LJ, Hartzell HC (1994) Molecular physiology of norepinephrine and serotonin transporters. *J Exp Biol* **196**: 263–281

Brown LY, Kottman AH, Brown S (2003) Immunolocalization of zic2 expression in the developing forebrain. *Gene Expression Patterns* **3**: 361–367

Butt CM, Zhao B, Duncan MJ, Debski EA (2002) Sculpting the visual map: the distribution and function of serotonin-1A and serotonin-1B receptors in the optic tectum of the frog. *Brain Res* **931**: 21–31

Analysis and quantification of axonal projections in the SC

Brains of mice whose retina was electroporated around the optic disc and the ratios of electroporation were comparable were used to quantify possible differences in the retinocollicular projections along the rostrocaudal axis of the SC. 'Comparable' was defined as having a retinal electroporation ratio <12% different. Sections of the SC of equivalent lateromedial levels were analysed. For each section, the rostrocaudal length of the SC was divided into six portions and fluorescence intensity in a circular area of constant size inside of each portion in contact with the collicular surface was measured using Image J. In the cases where only the caudal portion of the SC was analysed at higher magnification, only one measurement was made. For each value, background fluorescence values were subtracted from absolute values. Then, value of absolute fluorescence was divided by the value of average fluorescence in the section, generating values of relative fluorescence. Data were statistically analysed with SPSS using a two-way ANOVA to evaluate the interactions between side of the colliculus (ipsi-contra) and the position of the projection or pharmacological treatment and position of the projection. All images were taken using DC500 camera (Leica) coupled to a Leica DM 5000B microscope. For quantification of the projections at the SC, pictures were taken with the ×5 objective except for the high magnification images that were taken using ×10 objective.

Supplementary data

Supplementary data are available at *The EMBO Journal* Online (<http://www.embojournal.org>).

Acknowledgements

We thank A Barco for help with microarrays analysis, sharing of the anti-Ach3 antibody, discussion of the results and critical reading of the paper, L Erskine for discussion and editing of the paper, C Mason for support, V Borrell and M Maravall for help with statistical analysis and Joan Galceran for advice on the luciferase assays. We are also grateful to the RIKEN BioResource Center (Japan) for providing the Zic2 mutant mice and KP Lesch and C Gross for the Sert mutant mice. We thank C Vegar for genotyping of the mice. We thank S Brown for generously share the Zic2 antibody and R Blakely for the SERT antibody. Research in the laboratory of EH is funded by grants from the Spanish Ministry of Science and Innovation (BFU2007-61831), CONSOLIDER-Ingenio Program (CDS2007-023) and a CDA from the Human Frontiers Science Program. CG-F is supported by a JAE-CSIC postdoctoral contract.

Conflict of interest

The authors declare that they have no conflict of interest.

- EphB1-dependent and -independent mechanisms. *Development* **135**: 1833–1841
- Gaspar P, Cases O, Maroteaux L (2003) The developmental role of serotonin: news from mouse molecular genetics. *Nat Rev Neurosci* **4**: 1002–1012
- Godement P, Salaun J, Imbert M (1984) Prenatal and postnatal development of retinogeniculate and retinocollicular projections in the mouse. *J Comp Neurol* **230**: 552–575
- Gonzalez EM, Penedo LA, Oliveira-Silva P, Campello-Costa P, Guedes RC, Serfaty CA (2008) Neonatal tryptophan dietary restriction alters development of retinotectal projections in rats. *Exp Neurol* **211**: 441–448
- Gu Q, Singer W (1995) Involvement of serotonin in developmental plasticity of kitten visual cortex. *Eur J Neurosci* **7**: 1146–1153
- Guillery RW (1969) An abnormal retinogeniculate projection in Siamese cats. *Brain Res* **14**: 739–741
- Heils A, Wichems C, Mossner R, Petri S, Glatz K, Bengel D, Murphy DL, Lesch KP (1998) Functional characterization of the murine serotonin transporter gene promoter in serotonergic raphe neurons. *J Neurochem* **70**: 932–939
- Herrera E, Brown LY, Aruga J, Rachel RA, Dolen G, Mikoshiba K, Brown S, Mason CA (2003) Zic2 patterns binocular vision by specifying the uncrossed retinal projection. *Cell* **114**: 545–557
- Huberman AD, Feller MB, Chapman B (2008) Mechanisms underlying development of visual maps and receptive fields. *Annu Rev Neurosci* **31**: 479–509
- Jennings KA, Loder MK, Sheward WJ, Pei Q, Deacon RM, Benson MA, Olverman HJ, Hastie ND, Harmar AJ, Shen S, Sharp T (2006) Increased expression of the 5-HT transporter confers a low-anxiety phenotype linked to decreased 5-HT transmission. *J Neurosci* **26**: 8955–8964
- Karlstrom RO, Trowe T, Klostermann S, Baier H, Brand M, Crawford AD, Grunewald B, Haffter P, Hoffmann H, Meyer SU, Muller BK, Richter S, van Eeden FJ, Nusslein-Volhard C, Bonhoeffer F (1996) Zebrafish mutations affecting retinotectal axon pathfinding. *Development* **123**: 427–438
- Kliot M, Shatz CJ (1985) Abnormal development of the retinogeniculate projection in Siamese cats. *J Neurosci* **5**: 2641–2653
- Leamey CA, Merlin S, Lattouf P, Sawatari A, Zhou X, Demel N, Glendinning KA, Oohashi T, Sur M, Fassler R (2007) Ten_m3 regulates eye-specific patterning in the mammalian visual pathway and is required for binocular vision. *PLoS Biol* **5**: e241
- Lin SL, Setya S, Johnson-Farley NN, Cowen DS (2002) Differential coupling of 5-HT(1) receptors to G proteins of the G(i) family. *Br J Pharmacol* **136**: 1072–1078
- Lopez de Armentia M, Jancic D, Olivares R, Alarcon JM, Kandel ER, Barco A (2007) cAMP response element-binding protein-mediated gene expression increases the intrinsic excitability of CA1 pyramidal neurons. *J Neurosci* **27**: 13909–13918
- Mazer C, Muneyyirci J, Taheny K, Raio N, Borella A, Whitaker-Azmitia P (1997) Serotonin depletion during synaptogenesis leads to decreased synaptic density and learning deficits in the adult rat: a possible model of neurodevelopmental disorders with cognitive deficits. *Brain Res* **760**: 68–73
- McLaughlin T, Hindges R, O'Leary DD (2003) Regulation of axial patterning of the retina and its topographic mapping in the brain. *Curr Opin Neurobiol* **13**: 57–69
- Mizugishi K, Aruga J, Nakata K, Mikoshiba K (2001) Molecular properties of Zic proteins as transcriptional regulators and their relationship to GLI proteins. *J Biol Chem* **276**: 2180–2188
- Nagai T, Aruga J, Minowa O, Sugimoto T, Ohno Y, Noda T, Mikoshiba K (2000) Zic2 regulates the kinetics of neurulation. *Proc Natl Acad Sci USA* **97**: 1618–1623
- Nicol X, Bennis M, Ishikawa Y, Chan GC, Reperant J, Storm DR, Gaspar P (2006) Role of the calcium modulated cyclases in the development of the retinal projections. *Eur J Neurosci* **24**: 3401–3414
- Nicol X, Voyatzis S, Muzerelle A, Narboux-Neme N, Sudhof TC, Miles R, Gaspar P (2007) cAMP oscillations and retinal activity are permissive for ephrin signaling during the establishment of the retinotopic map. *Nat Neurosci* **10**: 340–347
- O'Neill GM, Fashena SJ, Golemis EA (2000) Integrin signalling: a new Cas(t) of characters enters the stage. *Trends Cell Biol* **10**: 111–119
- Penn AA, Riquelme PA, Feller MB, Shatz CJ (1998) Competition in retinogeniculate patterning driven by spontaneous activity. *Science* **279**: 2108–2112
- Petros TJ, Shrestha BR, Mason C (2009) Specificity and sufficiency of EphB1 in driving the ipsilateral retinal projection. *J Neurosci* **29**: 3463–3474
- Pfeiffenberger C, Cutforth T, Woods G, Yamada J, Renteria RC, Copenhagen DR, Flanagan JG, Feldheim DA (2005) Ephrin-As and neural activity are required for eye-specific patterning during retinogeniculate mapping. *Nat Neurosci* **8**: 1022–1027
- Pham TA, Rubenstein JL, Silva AJ, Storm DR, Stryker MP (2001) The CRE/CREB pathway is transiently expressed in thalamic circuit development and contributes to refinement of retinogeniculate axons. *Neuron* **31**: 409–420
- Plas DT, Visel A, Gonzalez E, She WC, Crair MC (2004) Adenylate cyclase 1 dependent refinement of retinotopic maps in the mouse. *Vision Res* **44**: 3357–3364
- Ravary A, Muzerelle A, Herve D, Pascoli V, Ba-Charvet KN, Girault JA, Welker E, Gaspar P (2003) Adenylate cyclase 1 as a key actor in the refinement of retinal projection maps. *J Neurosci* **23**: 2228–2238
- Rebsam A, Petros TJ, Mason CA (2009) Switching retinogeniculate axon laterality leads to normal targeting but abnormal eye-specific segregation that is activity dependent. *J Neurosci* **29**: 14855–14863
- Rebsam A, Seif I, Gaspar P (2002) Refinement of thalamocortical arbors and emergence of barrel domains in the primary somatosensory cortex: a study of normal and monoamine oxidase a knock-out mice. *J Neurosci* **22**: 8541–8552
- Rebsam A, Seif I, Gaspar P (2005) Dissociating barrel development and lesion-induced plasticity in the mouse somatosensory cortex. *J Neurosci* **25**: 706–710
- Rhoades RW, Bennett-Clarke CA, Lane RD, Leslie MJ, Mooney RD (1993) Increased serotonergic innervation of the hamster's superior colliculus alters retinotectal projections. *J Comp Neurol* **334**: 397–409
- Rossi FM, Pizzorusso T, Porciatti V, Marubio LM, Maffei L, Changeux JP (2001) Requirement of the nicotinic acetylcholine receptor beta 2 subunit for the anatomical and functional development of the visual system. *Proc Natl Acad Sci USA* **98**: 6453–6458
- Salichon N, Gaspar P, Upton AL, Picaud S, Hanoun N, Hamon M, De Maeyer E, Murphy DL, Mossner R, Lesch KP, Hen R, Seif I (2001) Excessive activation of serotonin (5-HT) 1B receptors disrupts the formation of sensory maps in monoamine oxidase a and 5-HT transporter knock-out mice. *J Neurosci* **21**: 884–896
- Sanchis-Segura C, Lopez-Atalaya JP, Barco A (2009) Selective boosting of transcriptional and behavioral responses to drugs of abuse by histone deacetylase inhibition. *Neuropsychopharmacology* **34**: 2642–2654
- Sarnyai Z, Sibille EL, Pavlides C, Fenster RJ, McEwen BS, Toth M (2000) Impaired hippocampal-dependent learning and functional abnormalities in mice lacking serotonin(1A) receptors. *Proc Natl Acad Sci USA* **97**: 14731–14736
- Schaeren-Wiemers N, Gerfin-Moser A (1993) A single protocol to detect transcripts of various types and expression levels in neural tissue and cultured cells: *in situ* hybridization using digoxigenin-labelled cRNA probes. *Histochemistry* **100**: 431–440
- Simon DK, O'Leary DD (1992) Development of topographic order in the mammalian retinocollicular projection. *J Neurosci* **12**: 1212–1232
- Sodhi MS, Sanders-Bush E (2004) Serotonin and brain development. *Int Rev Neurobiol* **59**: 111–174
- Sretavan DW, Shatz CJ, Stryker MP (1988) Modification of retinal ganglion cell axon morphology by prenatal infusion of tetrodotoxin. *Nature* **336**: 468–471
- Stellwagen D, Shatz CJ, Feller MB (1999) Dynamics of retinal waves are controlled by cyclic AMP. *Neuron* **24**: 673–685
- Upton AL, Ravary A, Salichon N, Moessner R, Lesch KP, Hen R, Seif I, Gaspar P (2002) Lack of 5-HT(1B) receptor and of serotonin transporter have different effects on the segregation of retinal axons in the lateral geniculate nucleus compared to the superior colliculus. *Neuroscience* **111**: 597–610
- Upton AL, Salichon N, Lebrand C, Ravary A, Blakely R, Seif I, Gaspar P (1999) Excess of serotonin (5-HT) alters the segregation of ipsilateral and contralateral retinal projections in monoamine oxidase A knock-out mice: possible role of 5-HT uptake in retinal ganglion cells during development. *J Neurosci* **19**: 7007–7024
- Williams RW, Hogan D, Garraghty PE (1994) Target recognition and visual maps in the thalamus of achiasmatic dogs. *Nature* **367**: 637–639

- Williams SE, Mann F, Erskine L, Sakurai T, Wei S, Rossi DJ, Gale NW, Holt CE, Mason CA, Henkemeyer M (2003) Ephrin-B2 and EphB1 mediate retinal axon divergence at the optic chiasm. *Neuron* **39**: 919–935
- Wolf BD, Chiba A (2000) Axon pathfinding proceeds normally despite disrupted growth cone decisions at CNS midline. *Development* **127**: 2001–2009
- Wong DT, Bymaster FP, Engleman EA (1995) Prozac (fluoxetine, Lilly 110140), the first selective serotonin uptake inhibitor and an antidepressant drug: twenty years since its first publication. *Life Sci* **57**: 411–441
- Wong DT, Horng JS, Bymaster FP, Hauser KL, Molloy BB (1974) A selective inhibitor of serotonin uptake: Lilly 110140, 3-(p-trifluoromethylphenoxy)-N-methyl-3-phenylpropylamine. *Life Sci* **15**: 471–479
- Xu Y, Sari Y, Zhou FC (2004) Selective serotonin reuptake inhibitor disrupts organization of thalamocortical somatosensory barrels during development. *Brain Res Dev Brain Res* **150**: 151–161



The EMBO Journal is published by Nature Publishing Group on behalf of European Molecular Biology Organization. This work is licensed under a Creative Commons Attribution-NonCommercial-Share Alike 3.0 Unported License. [<http://creativecommons.org/licenses/by-nc-sa/3.0/>]